



Cosmogenic nuclide-derived downcutting rates of canyons within large limestone plateaus of southern Massif Central (France) reveal a different regional speleogenesis of karst networks

Oswald Malcles¹, Philippe Vernant¹, David Fink², Gaël Cazes¹, Jean-François Ritz¹, Toshiyuki Fujioka³,
5 Jean Chéry¹

¹Géosciences Montpellier, Université de Montpellier, CNRS, Montpellier, France

²Australian Nuclear Science and Technology Organisation, Sydney, Australia

³Centro Nacional de Investigación sobre la Evolución Humana (CENIEH), Burgos, Spain

Correspondence to: Oswald Malcles (oswald.malcles@umontpellier.fr)

10 **Abstract.** We present 27 new burial ages based on ²⁶Al/¹⁰Be ratios of terrestrial cosmogenic radionuclides measured in clasts
and sediments deep within 12 caves in the southern Massif Central, France. Our results together with previously published
burial ages, verifies that cave morphogenesis has been continuously active in this region for at least the past ~6 Myrs.
Combining sample burial ages with their associated cave elevation above modern stream bed gives a mean regional incision
rate of 88 ± 5 m/Ma for the Grands Causses area. South of the Cevennes Fault zone bordering the Grands Causses, the
15 incision rate is 43 ± 5 m/Ma, suggesting that this difference might be accommodated by the fault zone. Sediment burial ages
from caves which are not located on river valley flanks or cliff walls are surprisingly too young relatively to the expected age
calculated using this regional average river incision rate. This suggests that the classical epigenic speleogenesis model that
presumes a direct correlation between cave level development and regional base level lowering does not apply for the study
area. Therefore, we propose that regional speleogenesis is mainly controlled by removal of ghost-rocks by regressive erosion
20 from river canyons to central parts of the plateaus, emptying incipient primokarst passages to create cave systems. Our
results suggest a continuum process from hypogene primokarst composed of ghost-rocks filled passages to epigene karst
dynamic emptying these passages and creating cave networks. We propose this is a major process in the southern Massif
Central that initiates the speleogenesis and control the geometry of the networks. In this region tiered karst cannot be
associated with major incising rivers but must be explained by former ghost-rocks (or hypogene) processes.

25 **1 Introduction – the origin of caves**

Speleogenesis has been an ongoing research topic for decades and debate on the spatial and temporal evolution of caves is
equally as old (Palmer, 2017). The current paradigm of epigenic speleogenesis (Fig. 1) includes: (1) steep vadose upstream
sections converging into (2) phreatic or epiphreatic sub-horizontal passages constrained by depth of the water table and (3)
subsequent groundwater emergence as springs at river valley floor (e.g. Ford and Williams, 2007, Audra and Palmer, 2013,
30 Harmand et al., 2017). In this epigenic model, the sub-horizontal passages, called “cave levels” or tiered karst, are assumed

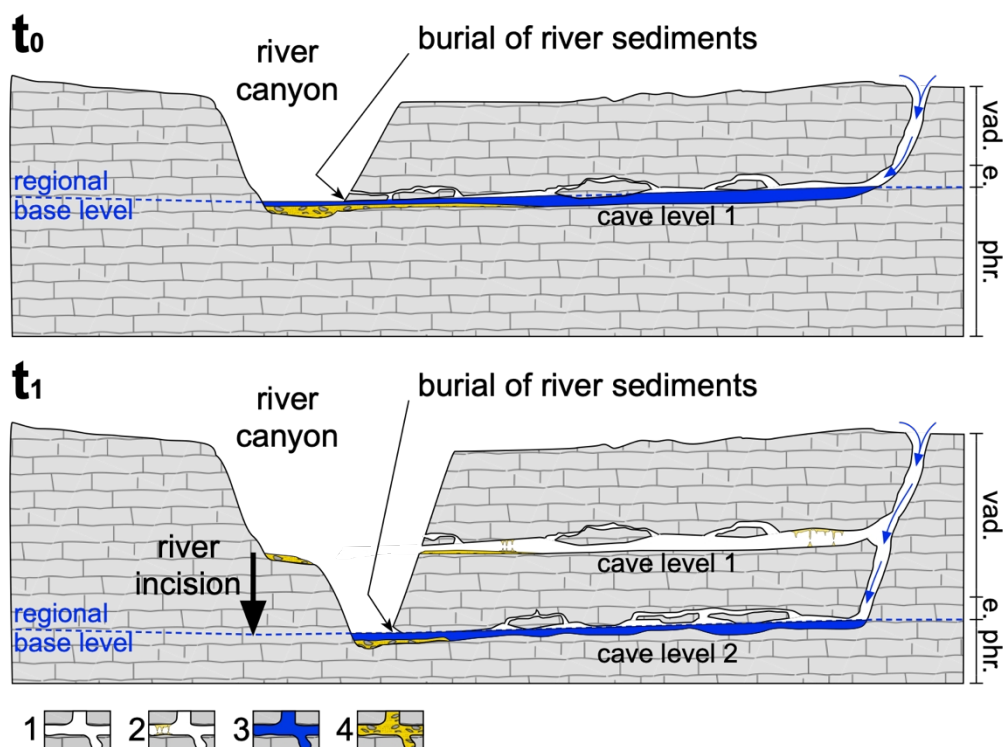


to have created via dissolution of bedrock during a prolonged period of base-level river stability. When river incision recommences, the water table lowers allowing formation of new passages and the previous generation of cave levels (usually higher in elevation) is then isolated from further fluvial occupation. Therefore, each cave level is considered to reflect a base level at a certain period of time in the past. This broadly accepted correlation between elevation of successive horizontal cave passages and fluvial evolution is commonly used to study speleogenesis and quantify incision rates (e.g. Granger et al 1997, Granger et al 2001, Stock et al., 2005, Harmand et al., 2017). The complication with this simple view of the epigenic speleogenesis paradigm (ESP) is that although groundwater discharge dissolves carbonates, it also simultaneously physically erodes and transports insoluble sections of bedrock. This process implies that large enough passages would need to exist prior to speleogenesis onset of sub-horizontal cave levels to avoid clogging of passages by insoluble bedrock fragments. To get around this problem, advocates of the conventional model postulate that open fractures in bedrock facilitates removal of soluble and insoluble products at the same time to allow speleogenesis. Other models have been proposed to explain speleogenesis, but they are commonly viewed as marginal processes “because these types of speleogenesis are not connected to a fluvial base level” Harmand et al. (2017). They include hypogenic cave formation mainly due to confined deep groundwater with a dissolution potential not related to surface processes (e.g. Klimchouk, 2012) or ghost-rock karstification (e.g. Dubois et al. 2014). Ghost-rock karstogenesis (also called phantomization) has been first described by Schmidt (1974) but mostly overlooked as a major karstification process. For Klimchouk (2017) it is a specific manifestation of hypogenic karstification. For others (e.g. Quinif, 2010, Dubois et al. 2014, Rodet, 2014) it can be a major regional karstification process involving a first stage of bedrock chemical weathering along least flow resistance paths (faults, fractures, bedding planes), with subsequent removal of the soluble matrix under low hydrodynamic conditions leaving the rock structure intact and essentially preserved with the more resistant insoluble matrix. At this stage, only incipient passages are formed along the weak flow paths (i.e. ‘ghost-like’ karstification) though often they can be misinterpreted as cave sediment infill. If hydrodynamic conditions change allowing rapid water flow, mechanical erosion of the ghost-rock will then preferentially open these weaker pre-existing paths and create caves. Whatever model of karstification is chosen, the passage formation is the result of 3 steps (e.g. Klimchouk, 2015): (1) the early stage corresponds to the widening of the flow path-ways; (2) the breakthrough phase which can be seen as the formation of efficient passages where the water can flow quickly and easily; (3) the last phase is when the main drains are well established allowing the stabilization of the system and the growth of the principal conduits. The main difference between the epigene karstification and the other processes is the relation to the regional base level. Epigene karst geometry is directly related to river incision dynamic, while hypogenic and ghost-rock karstification occur below the base level and subsequent tiered karst geometries cannot be interpreted in terms of river entrenchment phases.

We investigate speleogenesis of the Grands Causses region, southern Massif Central, France (Fig. 2). We apply the pioneering methods of Granger et al. (1997) using terrestrial cosmogenic radionuclide (TCN) $^{26}\text{Al}/^{10}\text{Be}$ ratios to estimate burial ages of quartz rich sediment and cobble cave infill together with detail cave mapping to generate river incision rates.



We spatially distinguish burial ages between caves opened on canyon edges to those centrally located in plateaus to test the
65 above models. Our results challenge the pervasive current ESP model of speleogenesis.



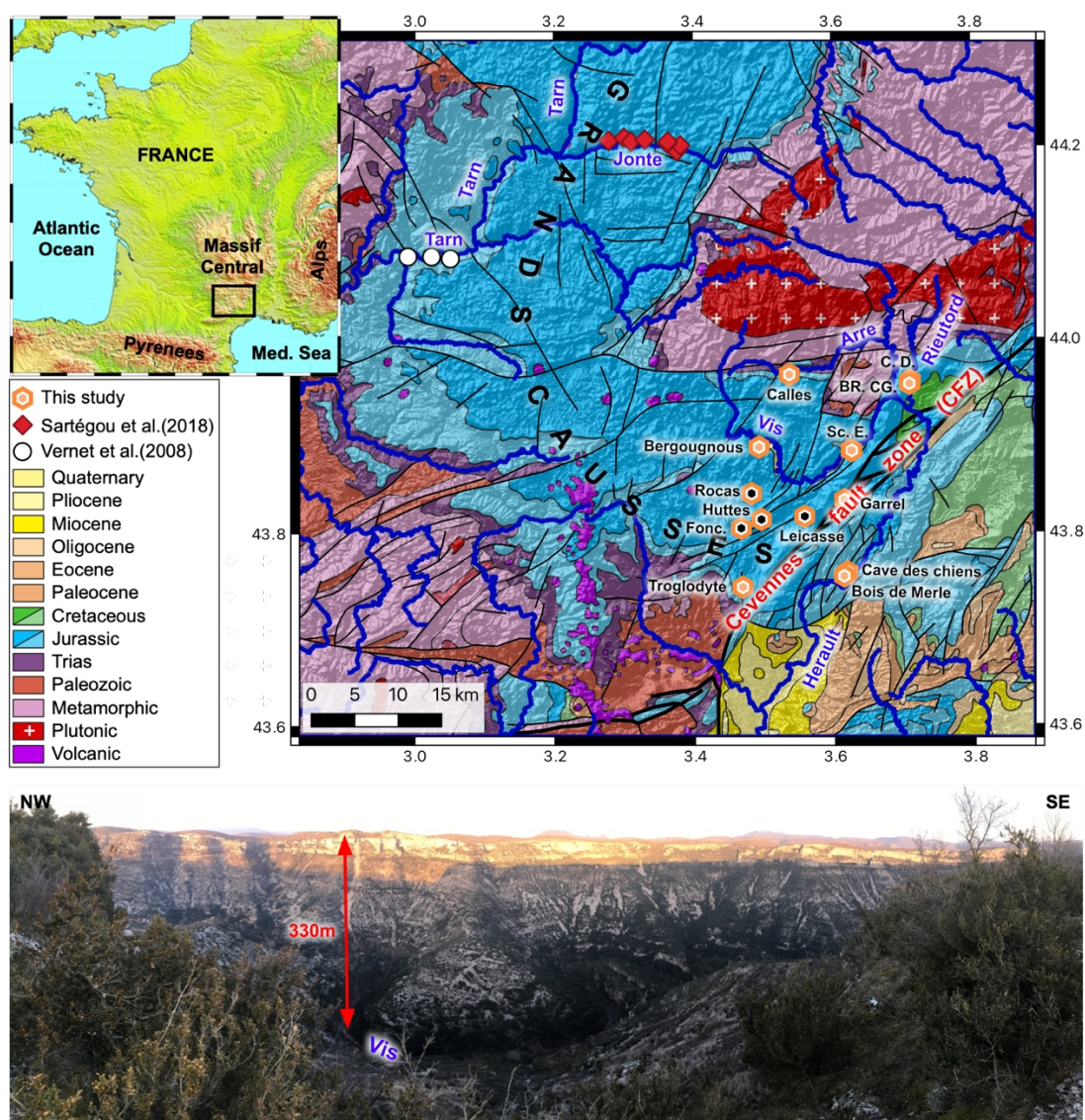
70 **Figure 1: Cave level development accordingly to the commonly accepted epiphreatic speleogenesis paradigm (ESP). Fig A (at $t = t_0$):** Water entering from the plateau dissolves and creates steep passages in the vadose zone (vad.) to connect to the epiphreatic (e.) and phreatic (phr.) zones where it forms sub-horizontal passages linked to the regional base level. **Fig B (at $t = t_1$):** subsequent river incision lowers the water table creating new cave levels (level 2) at the regional base level. Previously formed (older) cave levels (level 1) become abandoned. 1. Karstic network; 2. Karstic network with speleothems; 3. Active hydrological flow; 4. Allochthonous alluvial deposits.

2 Geology and Plio-Quaternary geomorphologic evolution of the Grands Causses

The Grands Causses region (Fig.2) is a large, elevated plateau of thick sub-horizontal Mesozoic carbonated series overlying
75 a Hercynian metamorphic and plutonic crystalline basement. Mean surface elevation is around 800m above sea level (a.s.l.) and its south-east margin is defined by a steep slope along the Cevennes Fault Zone (CFZ). The latest activity of this inherited major fault system according to Seranne et al. (2002) is an uplift of the north-west sector during the Serravalien/Tortonien (prior to ca. 8 Ma). Several rivers have their upper riverbeds and sources within crystalline areas (granite and schists). Their lower riverbeds carve deeply into the limestones on their journey to the Mediterranean Sea or the
80 Atlantic Ocean sculpting canyons that can be up to 400m deep (Fig. 2). Incision rates and timing of canyon production are



85 ~8 Ma (Sartégou et al. 2018).



90

Figure 2: Top: Simplified geological map of the study area and sample locations. The metamorphic and plutonic bedrock provide quartz rich sediments to the Tarn, Jonte, Arre, Rieutord, Vis and Hérault rivers. Darker colors for Jurassic and Cretaceous indicate thick limestone formations, lighter colors are for marls and thinner limestone formations. Sample site symbols with black hexagons (Fonc, Huttes, Rocas, and Leicasse) indicate the sampled cave is located away from the river canyons within a central section of the plateau Sc.: Scorpions, E.: Escoutet, BR.: Bord de Route, CG.: Camp de Guerre, C.: Cuillere, D.: Dugou, Fonc.: Fonctionnaire. Bottom: Photography of the Vis canyon located close from the Bergougounous sample.



3 Terrestrial Cosmogenic Nuclide (TCN) burial dating

We use TCN burial ages ($^{26}\text{Al}/^{10}\text{Be}$) to quantify regional incision rates. The method (Granger et al. 1997) uses the $^{26}\text{Al}/^{10}\text{Be}$ ratio produced by cosmic ray bombardment of subaerially exposed rocks, whereby after erosion and via fluvial transport, the irradiated quartz rich grains or cobbles are deposited and stored in cave systems. Here production ceases and the initial $^{26}\text{Al}/^{10}\text{Be}$ ratio decreases due to differential decay of the shorter lived ^{26}Al . We sampled quartz-rich alluvium and small cobbles in 8 new caves and resampled 4 others after previous studies (Malcles et al., 2020a, 2020b) for a total of 27 samples. The inventory includes 3 new Mediterranean Sea tributaries.

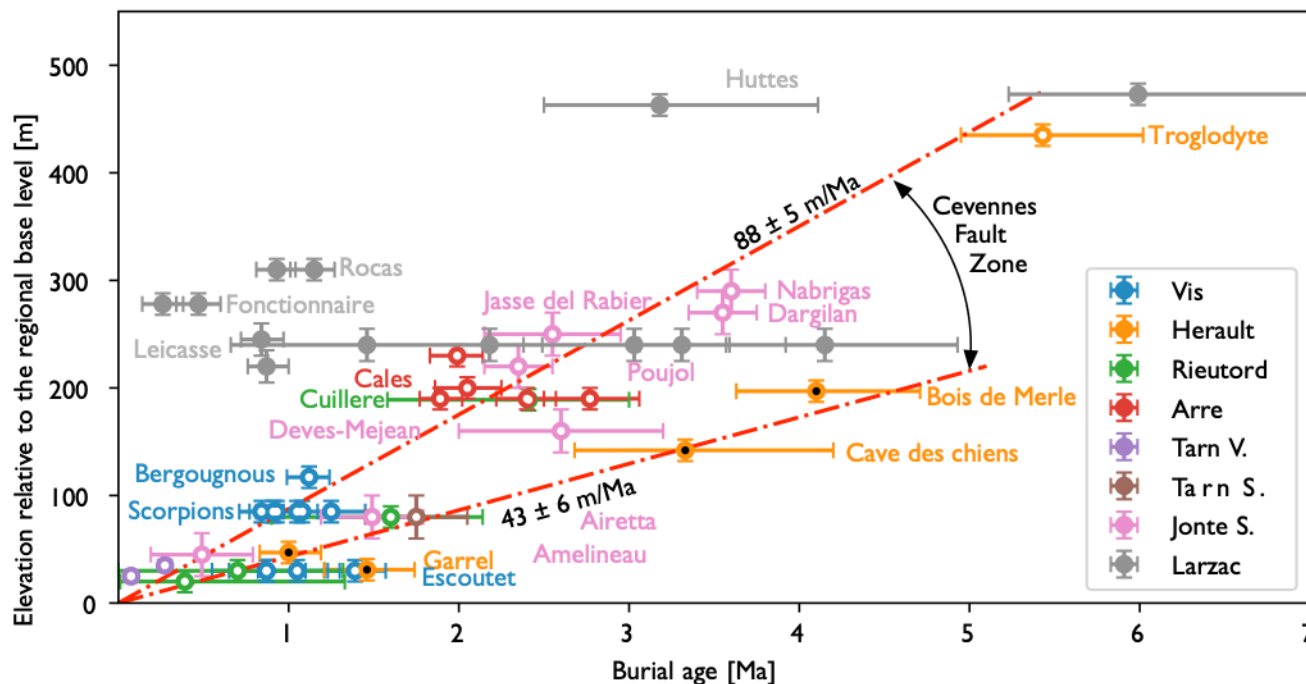
100 The samples are crushed, sieved, and processed with several selective chemical dissolutions to obtain pure quartz (Khol and Nishiizumi, 1992). After final HF etchings (suppression of $^{10}\text{Be}_{\text{atmo}}$), the samples are dissolved and Be and Al are separated by ion exchange chromatography and selective precipitations. BeO and Al_2O_3 mixed with Nb and Ag respectively are measured by the SIRIUS Accelerator Mass Spectrometer (Wilcken et al., 2019). AMS results for this study samples are normalized to standards KN-5-4 and KN-4-4 for Be and Al respectively (Nishiizumi et al., 2007) and corrected for blanks. 105 Final uncertainties for ^{10}Be and ^{26}Al concentrations include AMS statistics, 2% (Be) and 3% (Al) standard reproducibility, 1% uncertainty in the Be carrier solution concentration, and 4% uncertainty in the natural Al measurement made by inductively coupled plasma optical emission spectrometry (ICP-OES), in quadrature. ^{10}Be and ^{26}Al concentrations and their uncertainties are given in supplementary material (Table S1).

Details on burial dating theory are given in several studies (e.g., Granger et al., 1997, Granger and Muzikar, 2001, Dunai, 110 2010). We perform a two steps grid search to find the combination of burial ages and paleo-denudation rates consistent with the measured ^{10}Be and ^{26}Al concentrations. In the first step we use a loose grid with burial ages ranging from 10kyrs to 10Myrs with 1000 values spaced evenly on a log scale and paleo-denudation rates from 0.1 to 1000 m/Ma with 200 values also spaced evenly on a log scale. We check if the obtained values for ^{10}Be are consistent with ^{26}Al , if not, it means the concentrations are inconsistent with a simple history of bedrock erosion then river transport and finally cave burial. In this case no burial age can be estimated. If a consistent set of values exists, then we perform a second grid search with tighter 115 intervals to compute the consistent set of burial ages and paleo-denudation rates. To compute the theoretical concentrations, we account for variability of the cosmic-ray flux and therefore the cosmogenic nuclide production using scaling factors. For the neutron contribution we use Lal (1991) scaling factors. For the muon contribution, accordingly to the latest propositions (Braucher et al., 2013, Balco, 2017) we do not use slow and fast muons, but rather use the simpler geographic scaling 120 method of Balco (2017). The obtained values are plotted on Figure 3 and given in supplementary material (Table S1), the best combination of burial age and paleo-denudation rate is the one leading to the smallest chi square value of the difference between the measured and computed ^{10}Be and ^{26}Al concentrations. Uncertainties are computed accordingly to the burial ages and paleo-denudation rates consistent with the measured concentrations.



125 4 Discussion

We present in Figure 3 the burial ages from this study combined with previous TCN studies (Sartégou et al., 2018, Malcles et al., 2020a) and OSL results for terraces of the Tarn River (Vernet et al. 2008). The nearest river defines the relative elevation of the sample compared to local base level.



130 Figure 3: Burial age vs. relative elevation to the local water table level for each sample. Caves not located on the flanks of river channel but in central plateau areas are in grey, all the other caves are adjacent to or on river flanks or canyon walls. Jonte S. and Tarn S. are $^{26}\text{Al}/^{10}\text{Be}$ results from Sartégou et al. (2018) and Tarn V. are OSL results for Tarn River terraces from Vernet et al. (2008). Unfilled data points indicate they were used to compute the incision rate NW of the CFZ and black filled data symbols are samples used for the incision rate SE of the CFZ.

135 4.1 Multiple samples in the same cave level

When large enough cobbles were available, we independently processed them to obtain several burial ages for the same alluvium layer (Scorpions, Escoutet and Leicasse). Depending on the cave, some individual burial ages are spread over a wide age range. The wider the range, the more likely the sediments experienced an initial stay in an alluvium surface layer before being later buried in the cave when the sediment were reworked. When we compute independent burial ages, we estimate the paleo basin-wide mean denudation rate from bedrock erosion is sufficiently large to render little to no variability in the initial $^{26}\text{Al}/^{10}\text{Be}$ (inheritance) ratio. In order to confirm thus assumption, we also use Balco and Rovey (2008) isochron method on these 3 sets of samples. Without surprise the samples with a limited dispersion in the individual burial age computations (Escoutet and Scorpions) show well constrained linear regressions of ^{26}Al vs. ^{10}Be concentrations with $R^2 > 0.91$. On the other hand, samples from the Leicasse have an ill constrained regression with a $R^2 < 0.2$. This also consistent



145 with the very large estimates of paleo-denudation rates for some of the sampled cobbles in the Leicasse, inconsistent with the
most of paleo-denudation rates (<50 m/Ma) which suggest no large variation of denudation rates over the last 4 Myrs (Fig.
4). Therefore, rather than using the isochron method we prefer to use the independent age estimates. This choice is also
supported by alluvium layers of variable thicknesses (<15m) reported on the plateaus, and we advocate that the dispersion in
the individual burial ages is related to the reworking of these sediments in the caves. For the Leicasse samples, the
150 conversion of TCN concentrations into burial ages is not straightforward. In this case the younger age is a better measure,
equal or older, of the true cave burial age (~0.8 Myrs) of the deposit since its $^{26}\text{Al}/^{10}\text{Be}$ initial ratio was the one less likely
perturbated. This sample with the younger age, was the one located closer to the surface in the surface deposited alluvium
layer prior to burial. The older age (~4 Myrs) is a better measure, equal or younger, of the emplacement of the alluvium layer
that was subsequently buried into the cave. This sample was the one located deeper in the surface alluvium layer before cave
155 burial. Reported layer thickness are usually less than 15m which implies post deposit combined ^{26}Al and ^{10}Be production and
decay. All the other burial ages should be use with great precaution, and we think that the excessively high paleo-denudation
rates point in this direction too (Fig. 4, Leicasse samples). Based on the cave locations in the Vis River channel, the
Scorpions and the Escoutet samples are less likely to be affected by the injection of previously deposited alluvium at the
surface than the Leicasse. The narrow dispersion of independent burial ages and paleo-denudation rates are consistent with
160 this observation. Therefore, we think that in the case of burial ages determination for cave alluviums, if several samples are
collected, independent ages should be computed and the younger one should be retained except if complications are expected
due to the presence of glaciers in the valleys, which is not the case in the study area.

4.2 Incision rates and southern Cevennes Fault zone activity

165 At first glance no clear pattern appears to be evident from Figure 3, however when one ranks distance to the nearest river
canyon or differentiates cave location relative to the CFZ, three sample sub-sets are evident. The first one, the set of Larzac
cave burial ages (Leicasse, Fonctionnaire, Rocas, Huttes; grey symbols in Fig 3) is located within the Larzac plateau (the
southern plateau of the Grands Causses plateaus). All these caves are distant by 2.5 to 5 km from the nearest river channel
and show no clear relationship between burial ages and relative elevations to the base level. We will discuss these caves in
170 part 4.3. The Larzac caves set aside, all other cave burial ages (non-grey symbols) in Fig 3 have cave entrances located in
river channels when base river level was at the cave entrance elevation. These caves located within the steep flanks of river
channels show a clear linear correlation - the higher the sample is above today's riverbed, the older its burial age (Fig. 3).
The Cevennes Fault Zone (CFZ) is a major geologic and topographic feature of the area. A first set of caves (Garrel, Bois de
Merle, Cave des chiens) resides south-east of the CFZ in a lower elevation limestone plateau ~300 m a.s.l. whilst the second
175 includes all the caves from the Arre, Jonte, Rieutord, Tarn and Vis valleys and the Troglodyte cave and lie north-west of the
CFZ in higher elevation plateaus (600-1000m a.s.l.). Using cave location relative to the CFZ to define our two populations
we obtain an incision rate of 43 ± 6 (1σ , $n=4$) m/Ma for those south-east, while all other samples to the north-west of the



CFZ lead to an incision rate of 88 ± 5 m/Ma (1σ , $n=32$) consistent with the local previous estimates from Jonte valley (Sartégou et al., 2018), and from Rieutord samples (Malcles et al., 2020a). The low differential incision rate between the two populations of ~ 40 m/Ma, if focused on the CFZ, could lead to earthquakes with long recurrence times, consistent with the unexpected 2019 Mw 4.9 Teil earthquake (Ritz et al., 2020).

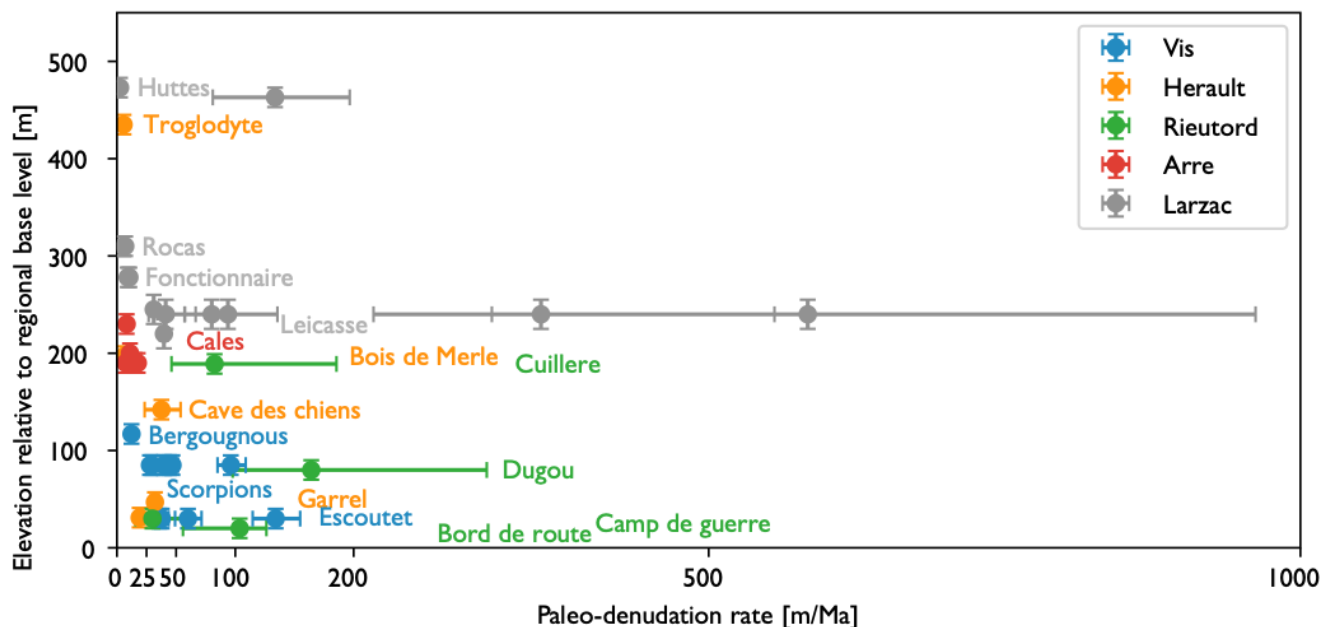


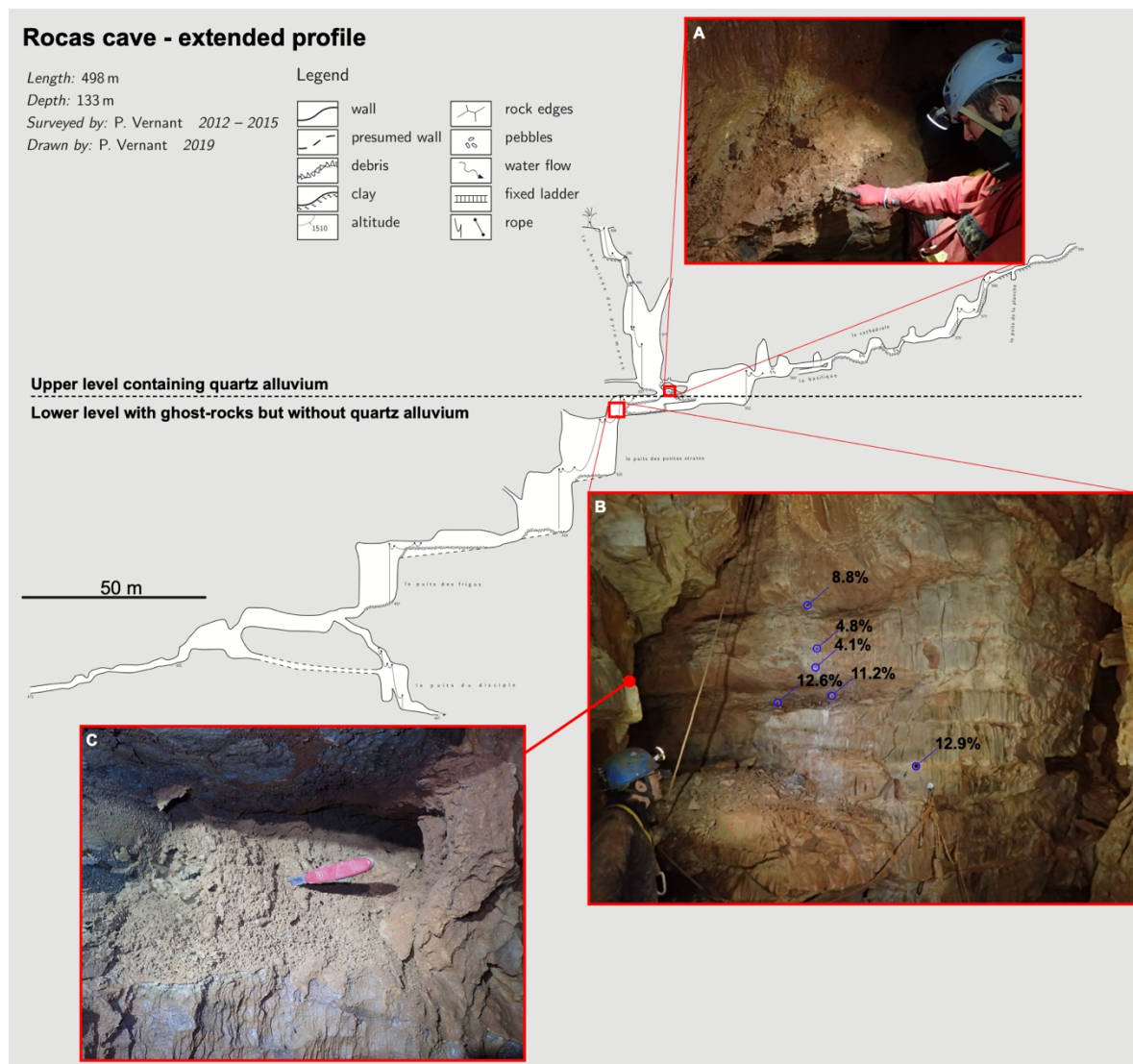
Figure 4: Paleo-denudation rate vs. relative elevation to the local water table level for each sample. Caves not located on the flanks of river channel but in central plateau areas are in grey, all the other caves are adjacent to or on river flanks or canyon walls. Jonte S. and Tarn S. are $^{26}\text{Al}/^{10}\text{Be}$ results from Sartégou et al. (2018) and Tarn V. are OSL results for Tarn River terraces from Vernet et al. (2008). Unfilled data points indicate they were used to compute the incision rate NW of the CFZ and black filled data symbols are samples used for the incision rate SE of the CFZ.

4.3 Speleogenesis implications: regressive erosion of altered rock zones

The unexpected result of diminished burial ages shown in Figure 3 came from the 4 Larzac plateau caves that are distant of at least 2.5km from any nearby river channel (Fig. 2). These caves have a clear classical tiered morphology that can be seen on the KARST3D database (KARST3D, 2019). Quartz rich sediments in Rocas are only located from -20m to -40m deep below the surface (555m - 575m a.s.l.) while the deepest part humanly accessible of the cave is at -130m (465m a.s.l.) (Fig. 5). In Fonctionnaire, the sediments are in the lowest of the 3 levels, at -75m below the surface (520 m a.s.l.). The Leicasse, which has 16km of mapped passages, alluvium is deposited in a ~ 1 km long passage at more that -140m below the surface (440 m a.s.l.). The 5 Leicasse quartz cobbles sampled in a common layer have burial ages ranging from 0.8 to 4.1 Myrs. The Huttes is a 200m long horizontal cave consisting of one level at 700m a.s.l. Using the youngest burial age from each of the 4 caves as the closest age for sediment emplacement leads to burial ages inconsistent with that expected from epigenic



speleogenesis paradigm (ESP) which would predict ages 2 to 4 ma older - or alternatively, a cave level elevation 150 to 250 m lower than recorded compared to the regional base level at the time of the deposit (Fig. 3).



200 **Figure 5: Extended profile of Rocas cave, with the lower limit of the upper level containing the quartz alluvium (A) and the lower level without quartz alluvium but with ghost rocks. Example of cave wall with higher porosities near the bedding planes showing the ghost-rocks (B), sometimes the porosity is so high that the rock structure is still apparent but fully pulverulent (C).**

The absence of sediments below 40m depth in Rocas indicates that the lower galleries formed less than a 1 million years ago, after emplacement of alluvium in the cave’s highest level. In this younger part of the cave, passages show morphologies similar to those reported for ghost-rock caves by Dubois et al. (2014) and Rodet (2014) and have preserved ghost-rock with
 205 porosities larger than 10% (Fig. 5). In the ESP model, precipitation moves downwards through plateau bedrock, enlarging fractures and bedding planes to form the cave gallery at the contemporary base level. In contrast the sub horizontal upper

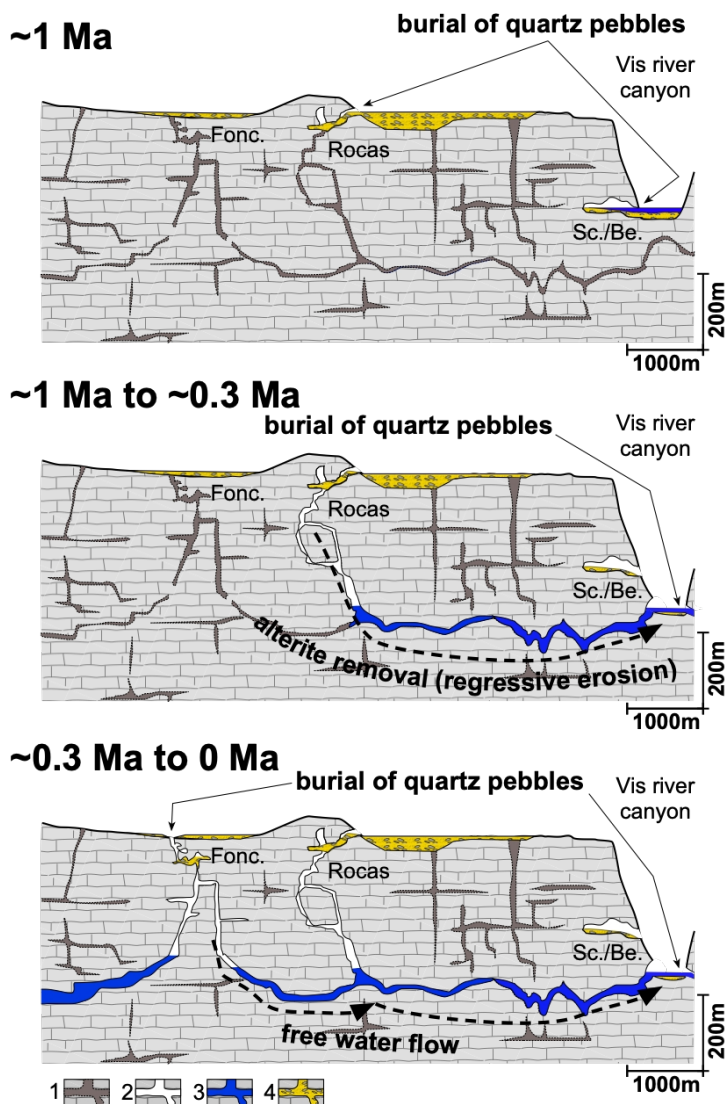


level of Rocas, which was filled with sediments 1 M years ago, is clearly not related to the base level of the Vis River, located at that time 250m lower, as registered by the same 1 Ma burial ages for the Scorpions and Bergougnous samples (Fig. 3). The same rationale applies to Fonctionnaire, Leicasse and Huttes caves and no impervious layers of marls are reported in the stratigraphic log at these cave elevations that could produce a perched karst. Furthermore, the wide range of the 5 cobble burial ages for the Leicasse (Fig. 3) and paleo-denudation rates (Fig. 4) are significantly larger than the ranges for all the caves located within river channels; (e.g., the 5 cobbles for Scorpions). We conclude that the sediments emplaced in Leicasse were not transported into the cave quickly nor directly by riverine fluvial processes, but they had resided on the plateau surface or at shallow depth at least for a period of 3 Myrs, the difference between the youngest and the oldest estimated burial age. Alluvium of former poljes are present at the surface of the Larzac plateau, they could be the source of the sediments that were later buried in the cave at the -140 m depth level without direct relation with the contemporary base level.

Areas of quartz rich sediments with large cobbles are still found at the surface of the plateau and therefore can be reworked into caves if they open nearby. Based on our results, we propose that contrary to the ESP, the speleogenesis of the Larzac plateau is driven by karstic regressive erosion from the canyon walls to the center of the plateau rather than by water working its way from the top of the plateau toward the valley. Given the rather quick formation of the caves, we propose that the passages were pre-structured by an alteration phase under low hydrodynamic gradient leading to numerous incipient passages full of ghost-rocks or isovolumic alterite (Fig. 6) retaining the original rock structure and called primokarst (Rodet, 2014). Ghost-rocks remain trapped in incipient passages where the water flow is practically absent since the boundaries of these incipient openings are impervious rocks, very thin fissures or bedding planes allowing only water and ions to slowly flow through. When the canyon cuts through one of these passages, it opens an outlet large enough to create a high hydrodynamic gradient allowing the mechanical removal of the ghost-rocks and creation of a new cave in a fairly short time as experienced in real time in Belgian quarries (Quinif, 2010). This is what occurred after 1 Ma for the lower part of the Rocas cave and around 0.3 to 0.5 million years ago, for the Fonctionnaire cave (Fig. 6). This regressive erosion works its way from the canyon walls toward the center of the plateau following the primokarst structures, and possibly creating deep sump (>100m) rather than river related tiered cave. Once the voids are opened the water can flow through quickly and modify the cave morphology, enlarging it and creating hydrodynamic markers like scallops. The specificity of the Larzac plateau with the layer of quartz rich alluvium at its surface has led to these unexpected results showing that cave levels, at least in this region, are related to preferential alteration levels subsequently emptied and, in some cases, enlarged by underground rivers when the primokarst was near or below the base level. Previous authors had proposed that ghost-rock removal could lead to large networks (Dubois et al., 2014, Quinif and Bruxelles, 2011), our results show that this process can be the major mechanism in the speleogenesis of large limestone plateaus like the Larzac (1000km²). They furthermore suggest that karstification can be a continuum process starting with hypogenic/ghost-rock karstification and continuing with



240 epigenetic karstification. The main difference with the widely admitted ESP model being that the network geometry is defined
by the hypogene/ghost-rock phase and not by the base level time evolution.



245 **Figure 6: Proposed Speleogenesis model for the cave in the center of the Larzac plateau based on the burial ages obtained in this study. The speleogenesis of the area is primarily due to alterite (ghost-rock) removal due to underground regressive erosion. 1. Primokarst filled with in-situ alterite, i.e. ghost-rock; 2. Karstic network; 3. Active hydrological flow; 4. Allochthonous alluvial deposits. Fonc.: Fonctionnaire cave, Sc./Be.:Scorpions and Bergounous caves.**



5 Conclusions

Combining 27 new burial ages with 23 previously published ages, we propose a mean regional river incision rate of 88 ± 5 m/Ma for the Grands Causses region and the first incision rate for the Hérault river of 43 ± 6 m/Ma, both over the last ~4 Myrs. These two regions are separated by the Cévennes Fault Zone, which could accommodate part of this differential as suggested by the Mw 4.9 Teil earthquake surface rupture ~100km further NE.

In addition, burial ages for alluvium deposited in the 4 caves located in the central Lézard plateau region which are all detached from river channel incision give unexpectedly younger ages by 1-3 Ma from that predicted by the conventional epigenic speleogenesis model. We conclude that the speleogenesis in the study area does not follow the widely accepted epigenic paradigm but is primarily due to regressive erosion of altered rocks. Once the river cuts through a primokarst by deepening its canyon the induced high waterflow can evacuate the ghost-rocks and quickly form new caves. Some of these caves can show several levels whose timing of construction are only related to the time of alteration of the rocks prior to the speleogenesis rather than being correlated to regional base level changes. We suggest that the already proposed ghost-rocks process for large karst networks genesis (Dubois et al., 2014, Quinif and Bruxelles, 2011) can also be applied at the scale of large limestone plateaus and could be the first stage of large void opening prior to the high waterflow hydrodynamic phase.

Competing interests

The contact author has declared that none of the authors has any competing interests.

Acknowledgments

We thank C. Mifsud, K. Stevens and S. Kotevski for their assistance during the sample processing. We thank K. Wilcken for assistance in some of the earlier AMS measurements. We also thank Y. Guessard, L. Bruxelles, M. Roux and L. Leterme for the identification of cave infilling or their help during sampling.

Financial support

O. Malcles benefited from a PhD grant provided by the French Ministère de l'Éducation Nationale de l'Enseignement Supérieur et de la Recherche.

This research was partially supported by ANSTO AINSE, (ANSTO - AP12168)



References

- Audra, P., and Palmer, A.N., 2013, 6.17 The Vertical Dimension of Karst: Controls of Vertical Cave Pattern, in *Treatise on Geomorphology*, Elsevier, p. 186–206, doi:10.1016/B978-0-12-374739-6.00098-1.
- 275
- Balco, G., and Rovey, C.W., 2008, An isochron method for cosmogenic-nuclide dating of buried soils and sediments: *American Journal of Science*, v. 308, p. 1083–1114, doi:10.2475/10.2008.02.
- Balco, G., 2017, Production rate calculations for cosmic-ray-muon-produced ^{10}Be and ^{26}Al benchmarked against geological calibration data: *Quaternary Geochronology*, v. 39, p. 150–173, doi:10.1016/j.quageo.2017.02.001.
- 280
- Braucher, R. et al., 2013, Determination of muon attenuation lengths in depth profiles from in situ produced cosmogenic nuclides: *Nuclear Instruments and Methods in Physics Research Section B: Beam Interactions with Materials and Atoms*, v. 294, p. 484–490, doi:10.1016/j.nimb.2012.05.023.
- 285
- Dubois, C. et al., 2014, The process of ghost-rock karstification and its role in the formation of cave systems: *Earth Science Reviews*, v. 131, p. 116–148, doi:10.1016/j.earscirev.2014.01.006.
- Dunai, T.J., 2010, *Cosmogenic Nuclides: Principles, Concepts and Applications in the Earth Surface Sciences.*: Cambridge University Press, 198 p.
- 290
- Fitzgerald, P.G., 1989, Uplift and formation of Transantarctic Mountains: Applications of apatite fission track analysis to tectonic problems: *International Geological Congress, 28th, Washington, D.C., Abstracts*, v. 1, p. 491.
- Ford, D., and Williams, P., 2007, *Karst Hydrogeology and Geomorphology: Ford/Karst Hydrogeology and Geomorphology*: West Sussex, England, John Wiley & Sons Ltd., doi:10.1002/9781118684986.
- 295
- Granger, D.E., Kirchner, J.W., and Finkel, R.C., 1997, Quaternary downcutting rate of the New River, Virginia, measured from differential decay of cosmogenic ^{26}Al and ^{10}Be in cave-deposited alluvium: *Geology*, v. 25, p. 107.
- 300
- Granger, D.E., and Muzikar, P.F., 2001, Dating sediment burial with in situ-produced cosmogenic nuclides: theory, techniques, and limitations: *Earth and Planetary Science Letters*, v. 188, p. 269–281, doi:10.1016/S0012-821X(01)00309-0.



305 Granger, D.E., Fabel, D., Palmer, A. N., 2001, Pliocene–Pleistocene incision of the Green River, Kentucky, determined from radioactive decay of cosmogenic ²⁶Al and ¹⁰Be in Mammoth Cave sediments. *GSA Bulletin* (2001) 113 (7): 825–836.

Harmand, D., Adamson, K., Rixhon, G., Jaillet, S., Losson, B., Devos, A., Hez, G., Calvet, M., and Audra, P., 2017, Relationships between fluvial evolution and karstification related to climatic, tectonic and eustatic forcing in temperate regions: *Quaternary Science Reviews*, v. 166, p. 38–56, doi:10.1016/j.quascirev.2017.02.016.

310 Karst3D Team Karst3D:; doi:10.15148/940C2882-49F1-49DB-A97E-12303CACE752.

Klimchouk, A., 2012, Speleogenesis, Hypogenic, in *Encyclopedia of Caves*, Elsevier, p. 748–765, doi:10.1016/B978-0-12-383832-2.00110-9.

315 Kohl, C.P., and Nishiizumi, K., 1992, Chemical isolation of quartz for measurement of in-situ -produced cosmogenic nuclides: *Geochimica et Cosmochimica Acta*, v. 56, p. 3583–3587, doi:10.1016/0016-7037(92)90401-4.

320 Lal, D., 1991, Cosmic ray labeling of erosion surfaces: in situ nuclide production rates and erosion models: *Earth and Planetary Science Letters*, v. 104, p. 424–439.

Malcles, O., Vernant, P., Chéry, J., Camps, P., Cazes, G., Ritz, J.-F., and Fink, D., 2020a, Determining the Plio-Quaternary uplift of the southern French Massif Central; a new insight for intraplate orogen dynamics: *Solid Earth*, v. 11, p. 241–258, doi:10.5194/se-11-241-2020.

325 Maleles, O., Vernant, P., Chéry, J., Ritz, J.-F., Cazes, G., and Fink, D., 2020b, Âges d'enfouissement, fantômes de roches et structuration karstique, cas de la vallée de la Vis (Sud de la France) : *Géomorphologie : relief, processus, environnement*, vol. 26 - n° 4 | 2020, 255-264, <https://doi.org/10.4000/geomorphologie.15043>.

330 Nishiizumi, K., Imamura, M., Caffee, M.W., Southon, J.R., Finkel, R.C., and McAninch, J., 2007, Absolute calibration of ¹⁰Be AMS standards: *Nuclear Instruments and Methods in Physics Research Section B: Beam Interactions with Materials and Atoms*, v. 258, p. 403–413, doi:10.1016/j.nimb.2007.01.297.

Palmer, A.N., 2017, *Cave Geology*, 4th edition 2017 454pp . Published by Cave Books ISBN 978 0 9397 48815.
335 Quinif, Y., 2010, *Fantômes de roche et fantômisations: essai sur un nouveau paradigme en karstogénèse*: Mons, Y. Quinif, *Karstologia Mémoires* 18, 196 p.



- Quinif, Y., and Bruxelles, L., 2011, L'altération de type « fantôme de roche » : processus, évolution et implications pour la karstification: *Géomorphologie : relief, processus, environnement*, v. 17, p. 349–358, doi:10.4000/geomorphologie.9555.
- 340 Ritz, J.-F., Baize, S., Ferry, M., Larroque, C., Audin, L., Delouis, B., and Mathot, E., 2020, Surface rupture and shallow fault reactivation during the 2019 Mw 4.9 Le Teil earthquake, France: *Communications Earth & Environment*, v. 1, p. 10, doi:10.1038/s43247-020-0012-z.
- 345 Rodet, J., 2014, The primokarst, former stages of karstification, or how solution caves can born: *Geologic Belgica*, v. 17, p. 58–65.
- Sartégou, A., Mialon, A., Thomas, S., Giordani, A., Lacour, Q., Jacquet, A., André, D., Calmels, L., Bourlès, D., Bruxelles,
350 L., Braucher, R., Leanni, L., and Team, Aster., 2018, When TCN meet high school students: deciphering western Cévennes landscape evolution (Lozère, France) using TCN on karstic networks, 4th Nordic Workshop on Cosmogenic Nuclides, 4-6 June 2018, doi:10.13140/RG.2.2.17907.37921.
- Schmidt, V.A., 1974, The paleohydrology of Laurel Caverns, Pennsylvania: *Proceedings of the 4th Conference on Karst
355 Geology and Hydrology*, Morgantown, W. Va., West Virginia Geological and Economic Survey, p. 123-128.
- Séranne, M., Camus, H., Lucazeau, F., Barbarand, J., and Quinif, Y., 2002, Polyphased uplift and erosion of the Cévennes (southern France). An example of slow morphogenesis: *Bulletin de la Société Géologique de France*, v. 173, p. 97–112, doi:10.2113/173.2.97.
- 360 Stock, G.M., Granger, D.E., Sasowsky, I.D., Anderson, R.S., and Finkel, R.C., 2005, Comparison of U–Th, paleomagnetism, and cosmogenic burial methods for dating caves: *Implications for landscape evolution studies*: v. 236, p. 388–403, doi:10.1016/j.epsl.2005.04.024.
- 365 Vernet, J., Mercier, N., Bazile, F., and Brugal, J., 2008, Travertins et terrasses de la moyenne vallée du Tarn à Millau (Sud du Massif Central, Aveyron, France) : datations OSL, contribution à la chronologie et aux paléoenvironnements: *Quaternaire*, p. 3–10, doi:10.4000/quaternaire.1422.
- Wilcken, K.M., Fujioka, T., Fink, D., Fülöp, R.H., Codilean, A.T., Simon, K., Mifsud, C., and Kotevski, S., 2019, SIRIUS
370 Performance: ¹⁰Be, ²⁶Al and ³⁶Cl measurements at ANSTO: *Nuclear Instruments and Methods in Physics Research Section B: Beam Interactions with Materials and Atoms*, v. 455, p. 300–304, doi:10.1016/j.nimb.2019.02.009.